CSMA 2026
17ème Colloque National en Calcul des Structures
18-22 Mai 2026, Presqu'île de Giens (Var)

Influence of the stress gradient on crack-growth initiation in variational phase-field models of fracture

A. Latyshev[1,2], J. S. Hale[1], C. Maurini[2]

[1] *Department of Engineering, Faculty of Science, Technology and Medicine, Université du Luxembourg, Luxembourg. andrey.latyshev@uni.lu, jack.hale@uni.lu*
[2] *Institut Jean Le Rond d'Alembert, Sorbonne Université, UMR CNRS 7190, France. corrado.maurini@sorbonne-universite.fr*

Résumé — This study investigates the influence of macroscopic stress gradient on crack-growth initiation within the variational phase-field model. By analyzing an edge-cracked plate under non-uniform tension, we demonstrate that the stress gradient stabilizes nucleation and significantly alters the size effect derived for uniform tensile loading. We identify a critical defect size that minimizes the initiation load, separating small, unstable flaws from large, stable ones that can be arrested. These findings highlight the interplay between material and structural length scales in predicting fracture onset.
Mots clés — phase-field, stress gradient, crack initiation, edge crack, size effect, brittle fracture.

1 Introduction

Variational phase-field models of fracture, frequently identified in the literature as a type of gradient damage or smeared crack model, provide a robust continuum framework that approximate sharp discontinuities as a smooth damage field. Originating from the variational approach to fracture proposed in [10], these methods regularize the fracture surface energy over a diffuse band of finite width, the size of which is governed by a characteristic length ℓ_{PF}. This formulation is mathematically related to the elliptic approximation of free-discontinuity problems developed by Ambrosio and Tortorelli (AT) [1, 2] and subsequently adapted for numerical fracture mechanics in [7, 8], and are hence known AT-type phase-field models. These models offer significant computational advantages ; they naturally predict complex fracture phenomena, including crack nucleation, propagation, and branching, solely through the minimization of a global energy functional. Consequently, they eliminate the need for ad-hoc failure criteria or complex algorithms for crack path tracking while maintaining reasonable numerical cost. In pure mode-I tension AT-type phase-field models are a reliable tool for predicting crack-growth initiation by reconciling stress-based and toughness-based criteria across scales, although they face challenges in accurately predicting nucleation under multiaxial mixed-mode or compression-dominated loading conditions, e.g. [17, 9].

This reconciliation between stress and toughness-based criteria yields the classical size effect ; small defects, relative to the characteristic length, are strength-controlled with an intrinsic tensile strength $\sigma_c \propto 1/\sqrt{\ell_{\mathrm{PF}}}$, whereas large defects are toughness-controlled and follow the Griffith model ; the onset curve transitions smoothly between these regimes. This behavior has been reproduced for the plate with central crack within a variational phase-field formulation under uniform loading, e.g. [13]. However, many practical configurations such as bending, wedge-splitting, or non-uniform boundary actuation, impose macroscopic stress gradients at the specimen scale, for which the classic size-effect framework is less firmly established. This motivates a central question that guides the present work ; how do stress gradients modify crack-growth initiation thresholds and reshape the size-effect landscape ?

A partial answer to this question was given by Pham, Laverne and Marigo [12], who analyzed a central crack in a sufficiently large solid subjected to prescribed, non-uniform tractions within a cohesive-zone model (CZM) and derived closed-form expressions for the evolution of the cohesive and non-cohesive crack lengths. In CZM, an intrinsic length arises from the traction–separation law, which sets the size of the fracture-process zone and enables size-effect behavior. Their analysis shows that a tensile stress gradient has a stabilizing effect on nucleation and growth ; nucleation loads increase, and crack advance can be arrested as the crack approaches a gradient-controlled length scale. These observations,

together with the presence of characteristic length scales in both CZM and phase-field formulations, inspire the present work to explore similar phenomena within a variational phase-field framework.

This work investigates the influence of a macroscopic stress gradient on crack-growth initiation within the AT1 phase-field model under mode-I-dominated non-uniform loading for a square plate with an edge crack. We demonstrate how stress gradients modify the size-effect landscape established in the previous study [13] and induce a stabilizing mechanism on damage nucleation. Furthermore, we introduce and analyze a critical crack size that minimizes the nucleation load.

2 Edge crack under stress gradient

2.1 Problem formulation

We study how a prescribed macroscopic stress gradient influences crack-growth initiation in a finite square domain D of height H and width $L = H$ in symmetric formulation containing an imperfection in the form of edge crack of length a that occupies a part of the left boundary, see Figure 1. The top and bottom edges of the domain are traction-free, whereas on the left boundary at $x = 0$ we impose the symmetry conditions as depicted on the Figure 1a. The right boundary at $x = L$ is subjected to a linearly varying displacement in the x-direction

$$u_t = t\left(1 - \frac{H-y}{\ell_\nabla}\right), \quad x = L,\ y \in [0, H], \tag{1}$$

where t is the quasi-static loading parameter and ℓ_∇ is the characteristic length that controls the stress-gradient, so that a finite $\ell_\nabla > 0$ induces a vertical stress gradient across the specimen height ; in particular, if $\ell_\nabla < H$, the lateral edges exhibit both tensile and compressive regions in linear elasticity. To avoid compression-dominated nucleation and isolate gradient effects we set $\ell_\nabla = 0.95\,H$.

(a) Geometry

(b) Regularized edge crack

FIGURE 1 – Edge crack in a finite plate under non-uniform tensile loading inducing a stress gradient (on the left) and initial damage field α_0 (on the right). The parameter ℓ_∇ controls the extent of the tensile region. Arrows indicate the direction of loading. The initial damage field α_0 regularizes the edge crack of length $a \approx 0.35H$ for zero loading $t = 0$ and $\ell_{\mathrm{PF}} = 0.05H$.

In this work, we employ the AT1 variational phase-field model for brittle fracture and seek a local minimizer of the following regularized energy functional

$$\mathcal{E}_{\ell_{\mathrm{PF}}}(\underline{u}, \alpha) = \frac{1}{2}\int_D \underline{\underline{\varepsilon}}(\underline{u}) : \underline{\underline{\underline{\underline{C}}}}(\alpha) : \underline{\underline{\varepsilon}}(\underline{u})\,\mathrm{d}\underline{x} \;+\; w_1 \int_D \left(w(\alpha) + \ell_{\mathrm{PF}}^2 \nabla\alpha \cdot \nabla\alpha\right)\,\mathrm{d}\underline{x}, \tag{2}$$

where $\underline{u}$ is the displacement vector field, $\underline{\underline{\varepsilon}}(\underline{u})$ the linearized second-rank strain tensor, $\underline{\underline{\underline{\underline{C}}}}(\alpha) = (1-\alpha)^2\,\underline{\underline{\underline{\underline{C}}}}$ the degraded fourth-rank elasticity tensor, $w(\alpha) = \alpha$ the local dissipation density, and $w_1 = 3G_c/(8\,\ell_{\mathrm{PF}})$ the specific fracture energy density with fracture toughness G_c. The parameter ℓ_{PF} is the regularization length and is interpreted as a material characteristic length scale. A detailed mathematical formulation of the local minimization problem of the AT1 model can be found, e.g. in [8, 13].

Our objective is to characterize the crack-growth initiation curve $a(t)$, which relates the crack length a of the edge crack initially presented in the domain to the onset loading level t, when this initial crack begins to grow. Under the present non-uniform loading (1), we exploit the symmetry of the problem

to assume a straight crack path and reconstruct $a(t)$ as follows : for a sequence of prescribed initial edge-crack lengths $a \in [0, 0.95H]$, we compute the minimal load t at which crack propagation initiates. Recording this onset load for each length yields the full initiation curve $a(t)$.

To compute each point on the initiation curve, we discretize $\mathcal{E}_{\ell_{\mathrm{PF}}}$ using finite elements and solve the coupled displacement-damage problem by alternating minimization under quasi-static loading. For a given crack length a, the initial edge crack is imposed as a regularized discontinuity by prescribing a nonzero damage field α_0 along the left boundary in the symmetric configuration (see Figure 1b) [11]. The initiation load t is then defined as the smallest load level at which the damage increment $\alpha - \alpha_0$ reaches unity at some point in the initially intact region (where $\alpha_0 = 0$), thereby signaling the onset of crack growth. Figure 2 illustrates the evolution of the energies and the maximum damage increment for a case with $a \approx 0.35H$ and $\ell_{\mathrm{PF}} = 0.05H$.

We discretize the displacement field $\underline{u}$ using quadratic (P2) elements and the damage field α using linear (P1) elements on a uniform mesh. For the smaller values of ℓ_{PF}, the mesh size is chosen to be less than $\ell_{\mathrm{PF}}/5$, which ensures mesh convergence of the phase-field approximation [8]. For the larger values ($\ell_{\mathrm{PF}}/H > 0.01$), the mesh is refined such that the P1 space contains approximately 2×10^4 degrees of freedom, ensuring sufficient accuracy of the finite element solution. All simulations use a unit square domain D with $H = L = 1\,\mathrm{m}$ and material parameters $E = 1\,\mathrm{MPa}$, $\nu = 0.3$, and $G_c = 0.1\,\mathrm{m}^{1/2}\,\mathrm{MPa}$. The computations are performed using the open-source finite-element library DOLFINx [3].

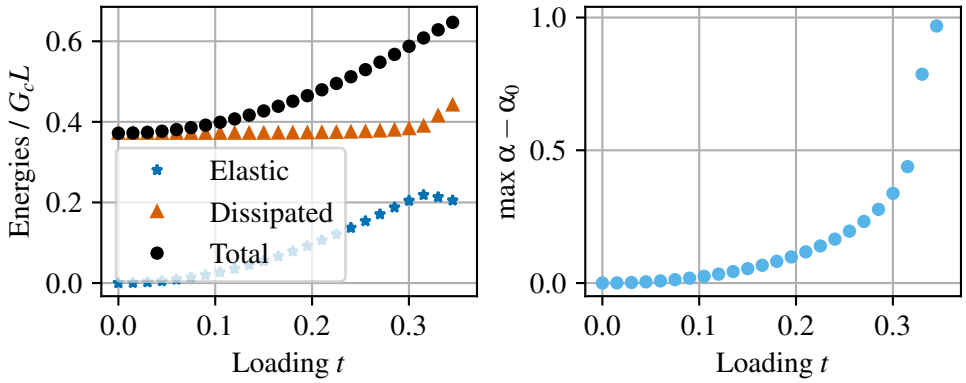

FIGURE 2 – Evolution of energies (left) and maximum damage increment $\alpha - \alpha_0$ (right). The initiation during quasi-static loading until crack-growth initiation. The initiation load is defined as the point where the damage increment $\alpha - \alpha_0$ reaches unity in the initially intact region (where $\alpha_0 = 0$). Parameters : $a \approx 0.35H$, $\ell_{\mathrm{PF}} = 0.05H$, $\ell_{\nabla} = 0.95H$.

Remark - time-discrete vs time-continuous formulations Although the phase-field model is presented here in a *time-continuous* quasi-static setting, the numerical results are computed in a *time-discrete* (incremental) manner by monotonically increasing the load parameter t. This distinction is immaterial for the present study because we only follow the response up to crack-growth initiation, which corresponds to a loss of stability of the equilibrium solution. Prior to this point, the evolution is smooth, and the incremental solutions converge to the time-continuous evolution. Rigorous analyses of stability and incremental schemes for phase-field models can be found in [5, 17].

2.2 Griffith model under stress gradient

In the brittle limit (i.e., as $\ell_{\mathrm{PF}} \to 0$), the phase-field functional $\mathcal{E}_{\ell_{\mathrm{PF}}}$ Γ-converges to the classical sharp-crack Griffith functional $\mathcal{E}^t$ [1], allowing us to compare phase-field nucleation predictions against the classical Griffith model. Under the loading (1) parameterized by t, we consider a sharp edge crack $\Gamma(a)$ of length a in the elastic plate D, whose total potential energy reads

$$\mathcal{E}^t(a) = \frac{1}{2} \int_{D \setminus \Gamma(a)} \underline{\underline{\varepsilon}}(\underline{u}^t(a)) : \underline{\underline{\underline{\underline{C}}}} : \underline{\underline{\varepsilon}}(\underline{u}^t(a)) \, \mathrm{d}\underline{x} + G_c a, \tag{3}$$

where $\underline{u}^t(a) = t\,\underline{u}^1(a)$ is the equilibrium displacement field for a fixed crack length a and load t, with $\underline{u}^1(a)$ the solution of the unit-load problem.

By introducing the energy release rate $G^t(a) := -\mathrm{d}\mathcal{E}^t(a)/\mathrm{d}a$, the quasi-static evolution of the crack length $a(t)$ is governed by the minimization of $\mathcal{E}^t(a)$ under the following constraints : (i) irreversibility $\dot{a} \geq 0$, (ii) stability $G^t(a) \leq G_c$, and (iii) energy balance $(G^t(a) - G_c)\dot{a} = 0$. We say that a pair (t_G, a_G) satisfies the *Griffith criterion* for the crack initiation, if under the constraints (i)–(iii) (t_G, a_G) is the minimizer of (3). The resulting dependence $t_G(a_G)$ serves as the baseline for comparison with phase-field predictions in the brittle limit.

Before analyzing the effects of stress gradients within the variational phase-field framework, we first illustrate the concept using the classical Griffith model for brittle fracture. The macroscopic stress gradient induced by the loading (1) can be approximated as a superposition of pure bending and uniform loading (in compression or tension depending on ℓ_∇). In this simplified scenario, the energy release rate admits a closed-form approximation, allowing us to derive the initiation load $t_G(a_G)$ directly from the Griffith criterion $G^{t_G}(a_G) = G_c$. Figure 3 compares this gradient-dependent solution ($\ell_\nabla > 0$) with the reference case of uniform tensile loading ($\ell_\nabla \to \infty$). The two loading scenarios exhibit distinct behaviors. For small flaws ($a \ll H$), both solutions coincide and predict infinite initiation loads, highlighting the well-known inability of the Griffith model to capture strength-driven nucleation $t_G = t_e$. However, for large flaws, the responses diverge. Under uniform tension, the initiation load decreases monotonically until failure ($a = H$). In contrast, under the combined bending and compression (which induces the stress gradient), the onset load eventually increases with crack length, tending towards infinity as the crack approaches a limiting length $a_{\mathrm{lim}} < H$. As will be shown later, this behavior persists in the phase-field model, while also capturing strength-driven nucleation.

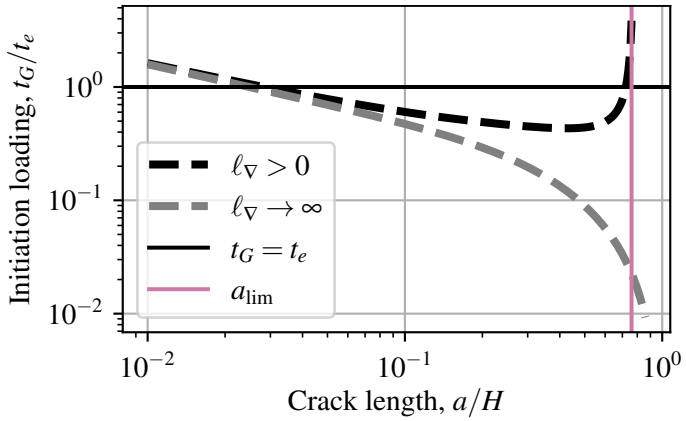

FIGURE 3 – Influence of the stress gradient represented by superposition of bending and compression ($\ell_\nabla > 0$) on the Griffith initiation curve $t_G(a_G)$ compared to the uniform loading ($\ell_\nabla \to \infty$) for the square plate with edge crack. The stress gradient induces a critical crack length a_{lim} beyond which crack growth cannot occur.

2.3 Crack-growth initiation and size effect under stress gradient

Now, we compare the evolution of $a(t)$ under spatially uniform loading ($\ell_\nabla \to \infty$) and non-uniform loading with a non-zero stress gradient ($\ell_\nabla > 0$). Results are presented in a log-log (a,t) plot with a normalized by the height H (bottom x-axis) and by the material length ℓ_{PF} (top x-axis), taking $\ell_{\mathrm{PF}} = H/100$. Figure 4 collects these curves and also reports the onset predicted by the Griffith criterion for the loading (1).

Under uniform loading ($\ell_\nabla \to \infty$), the curves reproduce a similar size effect to the well-known one titled as the "type 2 scaling law" by Bažant [6], namely small cracks ($a \ll \ell_{\mathrm{PF}}$) onset according to the material strength $t = t_e$, while large cracks ($a \gg \ell_{\mathrm{PF}}$) follow the Griffith criterion $t = t_G$, with a smooth transition between regimes (blue squares in Fig. 4). This behavior for variational phase-field models was reported in [13] for the first time. Unlike in the classical type 2 size-effect, our displacement-controlled setup introduces noticeable boundary effects for large cracks in a finite plate, so the onset t departs from the ideal Griffith curve for an edge crack in a finite plate (gray in Fig. 4). We also note that the

Griffith model overestimates the initiation load for small cracks, whereas the phase-field model, through its intrinsic length ℓ_{PF}, naturally captures the strength-governed onset.

With a nonuniform loading ($\ell_\nabla > 0$), the size-effect landscape changes markedly for large cracks. While the small and transitional regimes ($a \lesssim \ell_{\mathrm{PF}}$) remain close to the uniform-loading case, the onset load for large cracks increases and tends to infinity as $a \to \ell_\nabla$, unlike the classical size effect where the required load decreases monotonically with crack length until failure. Moreover, $a(t)$ exhibits snap-back under monotonic loading ; sufficiently small initial cracks a_0 (cf. Figure 4) jump to a larger $a(t)$ at onset, whereas sufficiently large initial cracks grow continuously along the upper branch of the loop. Despite these changes, the large-crack regime remains governed by Griffith, with $a(t)$ approaching the Griffith solution $t = t_G$ as $a \to \ell_\nabla$. These results qualitatively mirror those observed in Section 2.2 for a simplified loading scenario combining bending and compression.

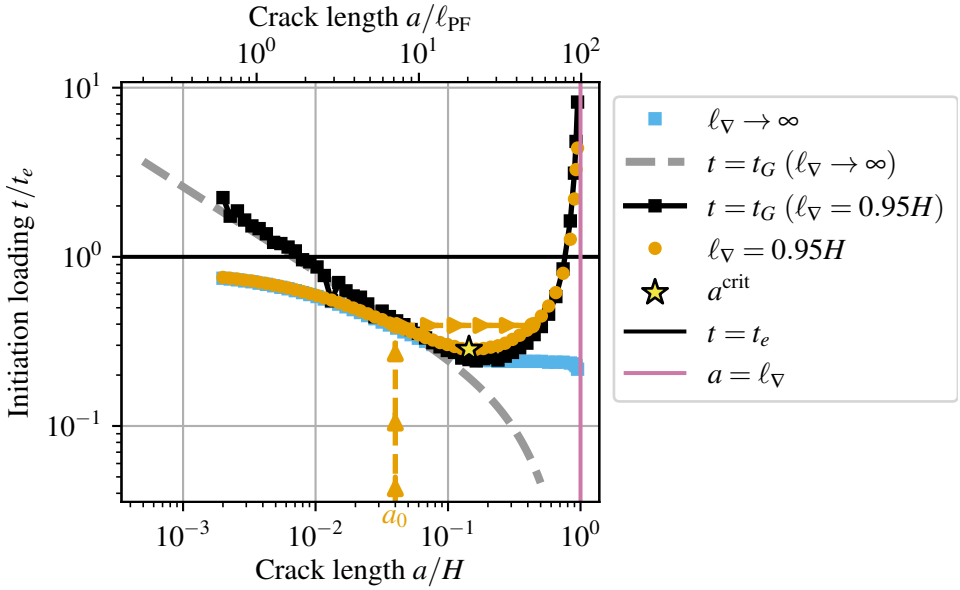

FIGURE 4 – Influence of the stress gradient (finite $\ell_\nabla = 0.95H$) on the size effect with respect to the uniform loading ($\ell_\nabla \to \infty$) for the finite plate with displacement-controlled boundary conditions with $\ell_{\mathrm{PF}} = H/100$.

Finally, the snap-back observed for finite ℓ_∇ reveals a minimum of the onset curve $t(a)$ (yellow star in Figure 4), absent under uniform loading. We denote this minimum as the *critical defect* a^{crit} and define it as

$$a^{\mathrm{crit}} = \arg\min\, t(a). \tag{4}$$

This minimum can be viewed as the worst imperfection because the specimen fails as soon as the load reaches $t(a^{\mathrm{crit}})$. It also provides a clear threshold to classify initial flaws ; we call cracks with $a < a^{\mathrm{crit}}$ *small*, and cracks with $a > a^{\mathrm{crit}}$ *large*.

2.4 Stabilizing role of the stress gradient and material length on crack-growth initiation

We organize the discussion around two length scales : the material length ℓ_{PF} and the gradient length ℓ_∇, and we compare responses to the perfect (defect-free) case with $a = 0$. We introduce the dimensionless parameter $\varepsilon := \sqrt{\ell_{\mathrm{PF}}/\ell_\nabla}$ to quantify their interplay, and we normalize the loading by t_{perfect}, i.e., we plot t/t_{perfect}. This choice highlights the relative drop of the onset load as the imperfection size a increases and is consistent with the classical size effect : for brittle materials (small ℓ_{PF}), $t_{\mathrm{perfect}} = t_e$, whereas for less brittle materials (large ℓ_{PF}) one has $t_{\mathrm{perfect}} \geq t_e$, enabling fair comparison across materials.

The material length ℓ_{PF} controls cohesive effects at the material scale [14] and thus can stabilize crack-growth initiation. Small ℓ_{PF} (small ε) corresponds to brittle behavior, whereas large ℓ_{PF} (large ε) corresponds to less brittle (more cohesive) behavior. Figure 5-left shows a/ℓ_∇ versus t/t_{perfect} for different ε, illustrating how ℓ_{PF} affects initiation under a stress gradient. As ε increases, (i) onset loads rise and (ii) the snap-back loop shrinks, smoothly transitioning from subcritical (unstable) to supercritical (stable) nucleation. For sufficiently large ε, the snap-back disappears and $a(t)$ becomes monotonic.

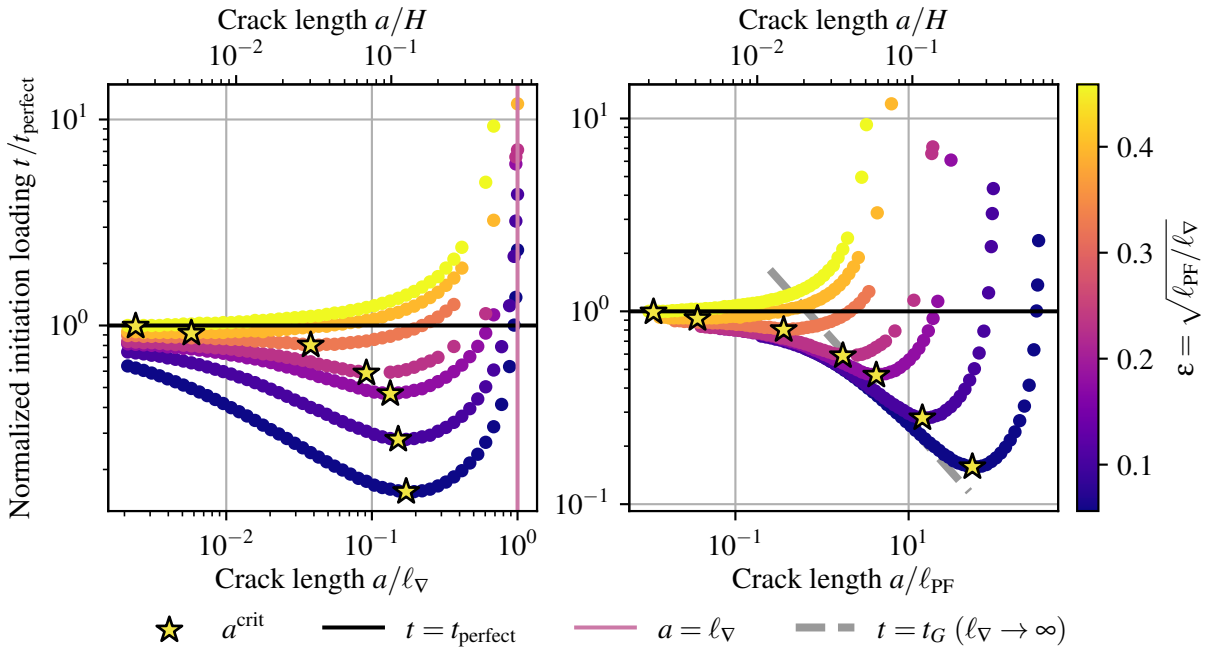

FIGURE 5 – Stabilizing role of the material length ℓ_{PF} (on the left) and the gradient length ℓ_∇ (on the right) on crack-growth initiation. The parameter $\varepsilon = \sqrt{\ell_{\text{PF}}/\ell_\nabla}$ quantifies the interplay between both length scales. Yellow stars mark the critical imperfection a^{crit} that minimizes the onset load $t(a)$.

The gradient length ℓ_∇ exerts a complementary stabilizing influence. Decreasing ℓ_∇ (larger ε) strengthens the macroscopic gradient and induces compression near the crack region, which inhibits initiation. This manifests as (i) a smaller snap-back loop, (ii) higher onset loads, and (iii) a reduced maximum crack length relative to the specimen height H. These trends are shown by plotting a/ℓ_{PF} versus t/t_{perfect} with increasing ε in Figure 5-right. Conversely, increasing ℓ_∇ (smaller ε) weakens the gradient, allowing larger cracks to develop and bringing the response closer to the uniform-loading case (cf. Figure 4).

Together, these stabilizing mechanisms are unified by the parameter ε, which governs the transition from unstable to stable crack-growth nucleation. As ε increases, the snap-back loop diminishes and the response becomes continuous. Consequently, even a brittle material (small ℓ_{PF}) can exhibit stable nucleation if subjected to a sufficiently strong stress gradient (small ℓ_∇), demonstrating the interplay between material and structural length scales.

2.5 Critical defect

In analogy with imperfection sensitivity in shell buckling [4, 15], we define the *critical defect* a^{crit} as the geometric imperfection that yields the minimum initiation load. The associated *fracture knockdown factor* $\eta(a^{\text{crit}}) = t(a^{\text{crit}})/t_{\text{perfect}}$ is the ratio of this minimum initiation load to the nucleation load of the intact solid.

Figure 6 shows the evolution of a^{crit} and η with the dimensionless parameter $\varepsilon = \sqrt{\ell_{\text{PF}}/\ell_\nabla}$. In the brittle limit ($\varepsilon \to 0$), η decreases significantly. For the smallest ε considered, the initiation load drops to less than 20% of the intact value, highlighting the high sensitivity of brittle materials to defects under stress gradients. In this regime, a^{crit} saturates to a value dependent only on ℓ_∇, matching the Griffith solution. Thus, for sufficiently brittle materials ($\ell_{\text{PF}} \to 0$), the Griffith model reliably predicts the critical defect size.

Conversely, as the material becomes less brittle (increasing ε), the knockdown factor η increases, decreasing sensitivity to imperfections. These results quantify the stabilizing effect of ℓ_{PF} discussed previously : increasing the material length scale transitions the response from a highly imperfection-sensitive subcritical behavior to a more stable supercritical one.

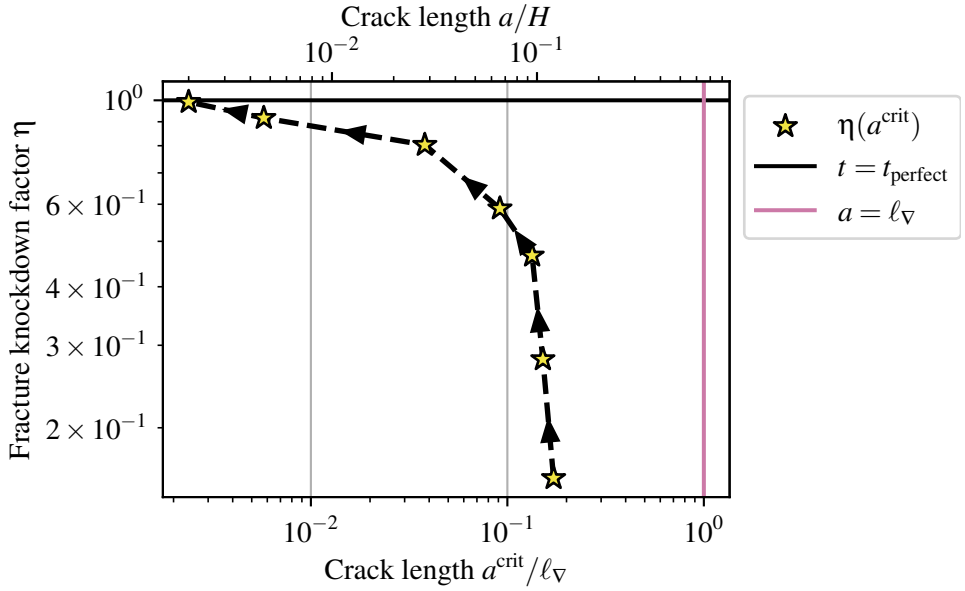

FIGURE 6 – The fracture knockdown factor $\eta(a^{\text{crit}}) = t(a^{\text{crit}})/t_{\text{perfect}}$ and the critical defect a^{crit} for various values of the dimensionless parameter $\varepsilon = \sqrt{\ell_{\text{PF}}/\ell_\nabla}$. Arrows indicate the direction of decreasing ε. For large ε, the material is less brittle and more resistant to initial imperfections. For small ε, behaviour is brittle delivering small knockdown factors.

3 Conclusion

Introduction of stress gradient in the vicinity of fracture reveals new features of crack initiation that cannot be observed in the common uniform loading tensile tests. Overall, the presence of the stress gradient plays a stabilizing mechanism on the crack onset by preventing the crack from growing due to presence of compression around the crack. This result was demonstrated for an edge crack in a square domain with displacement-controlled loading using the AT1 phase-field model.

When compared to the uniform loading case, the presence of the stress gradient allows to introduce a *critical imperfection* a^{crit} that, under monotonic loading, sorts the initial cracks into two categories :

1. large cracks $a > a^{\text{crit}}$, which (i) grow continuously approaching ℓ_∇ (Figure 4); (ii) follow the Griffith criterion for brittle materials; (iii) are arrested at $a \to \ell_\nabla$, unlike in the uniform loading case, where cracks grow unboundedly until specimen failure;
2. small cracks $a < a^{\text{crit}}$, which (i) propagate brutally by jumping to the upper part of the loop where $a \to \ell_\nabla$ (Figure 4); (ii) nucleation follows material strength and transitional parts of the size effect similar to uniform loading;

These findings and analysis of the size-effect under stress gradient reveal that the importance of accounting for gradient effects depends critically on the defect size relative to a^{crit}. For large cracks, stress gradients significantly influence crack initiation, but the classical Griffith model remains sufficient when the material behavior is brittle ($\ell_{\text{PF}} \ll H$). Conversely, for small or transitional flaws ($a < a^{\text{crit}}$), the response qualitatively resembles uniform loading, and a phase-field model becomes essential. This is particularly true for brittle materials, which exhibit the highest sensitivity to such defects, as evidenced by the smallest values of the fracture knockdown factor η. In this regime, the Griffith model fails to capture strength-driven nucleation.

A further key finding is that both the material length ℓ_{PF} and the stress gradient length ℓ_∇ independently influence crack initiation, either stabilizing or destabilizing the response. This interplay is captured by the dimensionless parameter $\varepsilon = \sqrt{\ell_{\text{PF}}/\ell_\nabla}$. As ε increases, the solid's resistance to crack initiation strengthens, leading to more stable fracture onset. This stabilization can be achieved through various mechanisms : a brittle material subjected to a sufficiently strong stress gradient, a less brittle material under moderate gradients, or a combination of reduced brittleness and enhanced gradients.

4 Funding

This research was funded in whole, or in part, by the Luxembourg National Research Fund (FNR), grant reference PRIDE/21/16747448/MATHCODA. For the purpose of open access, and in fulfilment of the obligations arising from the grant agreement, the author has applied a Creative Commons Attribution 4.0 International (CC BY 4.0) license to any Author Accepted Manuscript version arising from this submission.

Références

[1] L. Ambrosio, V. M. Tortorelli. *Approximation of Functional Depending on Jumps by Elliptic Functional via t-convergence*, Communications on Pure and Applied Mathematics, 43(8) :999–1036, 1990.

[2] L. Ambrosio. *On the Approximation of Free Discontinuity Problems*, Boll. Un. Mat. Ital., B, 7 :105–123, 1992.

[3] I. A. Baratta, J. P. Dean, J. S. Dokken, M. Habera, J. S. Hale, C. N. Richardson, M. E. Rognes, M. W. Scroggs, N. Sime, G. N. Wells. *DOLFINx : The next Generation FEniCS Problem Solving Environment*, 2023.

[4] J. W. Hutchinson, R. C. Tennyson, D. B. Muggeridge. *Effect of a Local Axisymmetric Imperfection on the Buckling Behavior of a Circular Cylindrical Shell under Axial Compression*, AIAA Journal, 9(1) :48–52, 1971.

[5] A. A. León Baldelli, C. Maurini. *Numerical Bifurcation and Stability Analysis of Variational Gradient-Damage Models for Phase-Field Fracture*, Journal of the Mechanics and Physics of Solids, 152 :104424, 2021.

[6] Z. P. Bažant. *Size Effect on Structural Strength : A Review*, Archive of Applied Mechanics, 69(9) :703–725, 1999.

[7] B. Bourdin, G. A. Francfort, J.-J. Marigo. *Numerical Experiments in Revisited Brittle Fracture*, Journal of the Mechanics and Physics of Solids, 48(4) :797–826, 2000.

[8] B. Bourdin, G. A. Francfort, J.-J. Marigo. *The Variational Approach to Fracture*, Journal of Elasticity, 91(1–3) :5–148, 2008.

[9] B. Bourdin, J.-J. Marigo, C. Maurini, C. Zolesi. *A Variational Approach to Fracture Incorporating Any Convex Strength Criterion*, arXiv :2506.22558, 2025.

[10] G. A. Francfort, J.-J. Marigo. *Revisiting Brittle Fracture as an Energy Minimization Problem*, Journal of the Mechanics and Physics of Solids, 46(8) :1319–1342, 1998.

[11] F. Loiseau, V. Lazarus. *How to Introduce an Initial Crack in Phase Field Simulations to Accurately Predict the Linear Elastic Fracture Propagation Threshold ?*, Journal of Theoretical, Computational and Applied Mechanics, 2025.

[12] T. H. Pham, J. Laverne, J.-J. Marigo. *Stress Gradient Effects on the Nucleation and Propagation of Cohesive Cracks*, Discrete and Continuous Dynamical Systems - S, 9(2) :557–584, 2016.

[13] E. Tanné, T. Li, B. Bourdin, J.-J. Marigo, C. Maurini. *Crack Nucleation in Variational Phase-Field Models of Brittle Fracture*, Journal of the Mechanics and Physics of Solids, 110 :80–99, 2018.

[14] H. Tran, H. B. Chew. *Cohesive Zone Interpretations of Phase-Field Fracture Models*, Journal of Applied Mechanics, 89 :121005, 2022.

[15] U. K. Ubamanyu, Z. Baizhikova, J.-L. Le, R. Ballarini, P. M. Reis. *A Numerical Study on the Buckling of Near-Perfect Spherical Shells*, Journal of Applied Mechanics, 92 :051003, 2025.

[16] X.-R. Wu, W. Xu. *Weight Function Methods in Fracture Mechanics : Theory and Applications*, Springer Nature Singapore, 2022.

[17] C. Zolesi, C. Maurini. *Stability and Crack Nucleation in Variational Phase-Field Models of Fracture : Effects of Length-Scales and Stress Multi-Axiality*, Journal of the Mechanics and Physics of Solids, 192 :105802, 2024.